Acta Cryst E
CRYSTALLOGRAPHIC COMMUNICATIONS
ISSN 2056-9890

Crystal structure and Hirshfeld surface analysis of 3,4-dihydro-2*H*-anthra[1,2-*b*][1,4]dioxepine-8,13-dione

Sofia Zazouli,[a]* Mohammed Chigr,[b] Ahmed Jouaiti,[a] Nathalie Kyritsakas[c] and El Mostafa Ketatni[b]

[a]Laboratory of Sustainable Development, Sultan Moulay Slimane University, Faculty of Sciences and Technologies, BP 523, 23000 Beni-Mellal, Morocco, [b]Laboratory of Organic and Analytical Chemistry, University Sultan Moulay Slimane, Faculty of Science and Technology, PO Box 523, Beni-Mellal, Morocco, and [c]Molecular Tectonics Laboratory, Université de Strasbourg, CNRS, CMC UMR 7140, F-67000 Strasbourg, France. *Correspondence e-mail: szazouli@gmail.com

Received 5 March 2020
Accepted 18 March 2020

Edited by W. T. A. Harrison, University of Aberdeen, Scotland

Keywords: crystal structure; anthraquinone; dioxepine; Schiff base; Hirshfeld surface analysis.

CCDC reference: 1991271

Supporting information: this article has supporting information at journals.iucr.org/e

The title compound, $C_{17}H_{12}O_4$, was synthesized from the dye alizarin. The dihedral angle between the mean plane of the anthraquinone ring system (r.m.s. deviation = 0.039 Å) and the dioxepine ring is 16.29 (8)°. In the crystal, the molecules are linked by C—H···O hydrogen bonds, forming sheets lying parallel to the *ab* plane. The sheets are connected through π–π and C=O···π interactions to generate a three-dimensional supramolecular network. Hirshfeld surface analysis was used to investigate intermolecular interactions in the solid-state: the most important contributions are from H···H (43.0%), H···O/O···H (27%), H···C/C···H (13.8%) and C···C (12.4%) contacts.

1. Chemical context

Anthraquinone derivatives, which are extracted from the seeds of the Rubiaceae family of shrubs, include alizarin (1,2-dihydroxyanthraquinone; $C_{14}H_8O_4$) and other polycyclic aromatic hydrocarbons. The colour of anthraquinone-based compounds can be modified by the type and position of the substituents attached to the anthraquinone nucleus (Nakagawa *et al.* 2017; Cheuk *et al.*, 2015; Tonin *et al.*, 2017). Besides their application as pigments or dyes in textile, photographic, cosmetic and other industries (Wang *et al.*, 2011), anthraquinone derivatives have been used for centuries for medical applications, for example, as laxatives (Oshio *et al.*, 1985), antioxidants (Yen *et al.*, 2000), antimicrobial (Xiang *et al.*, 2008; Yadav *et al.*, 2010) and anitiviral (Alves *et al.*, 2004) agents. Their redox properties and cytotoxicity have been investigated recently (Okumura *et al.*, 2019). Anthraquinone derivatives exhibit various applications in supramolecular and electro-analytical chemistry (Czupryniak *et al.*, 2012).

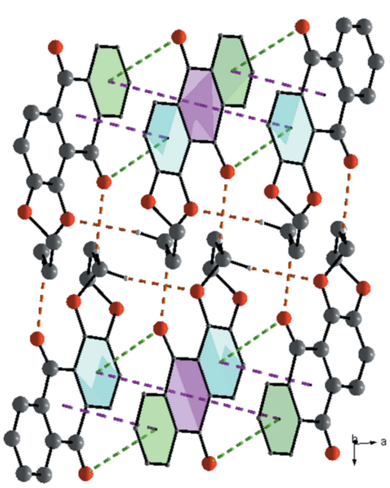

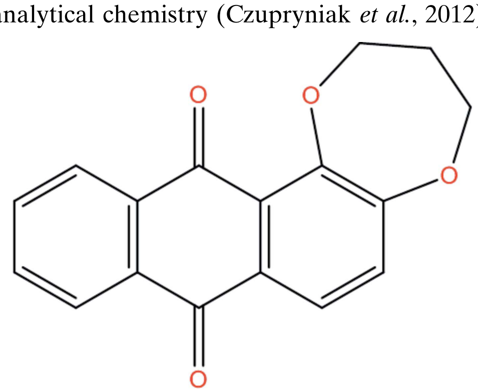

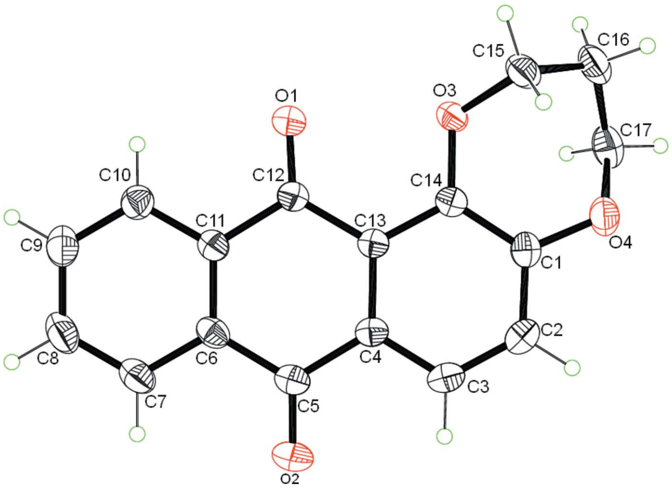

Figure 1
The molecular structure of (I) with displacement ellipsoids drawn at the 50% probability level.

As part of our studies in this area, the synthesis and structure of the title compound, (I), are described along with a detailed analysis of its supramolecular associations through an analysis of the Hirshfeld surfaces.

2. Structural commentary

Compound (I) crystallizes in space group $P2_1/n$ with one molecule in the asymmetric unit: it consists of three fused six-membered rings and one seven-membered ring as shown in Fig. 1. The fused-ring system is close to planar with an r.m.s. deviation for all non-hydrogen atoms of 0.039 Å (the dihedral angle between the aromatic rings of the anthraquinone unit and the central ring range from 1.5 to 1.9°). The dioxepine ring is inclined to the mean plane of the anthraquinone ring system by 16.29 (8)°.

A puckering analysis of the seven-membered ring yielded the parameters $q2$ = 0.896 (2) Å, φ_2 = 113.50 (12)°, q_3 = 0.358 (2) Å, and φ_3 = 217.8 (3)°. These metrics indicate that the ring adopts a screw boat conformation. The C—O and C=O bond lengths lie within the ranges 1.355 (2)–1.457 (2) Å and 1.216 (2)–1.226 (2) Å, respectively, confirming their single and double-bond character.

3. Supramolecular features

In the extended structure of (I), C15—H15*B*···O1 hydrogen bonds form inversion dimers with an $R_2^2(14)$ ring motif. Adjacent dimers are linked by C15—H15*A*···O3 contacts,

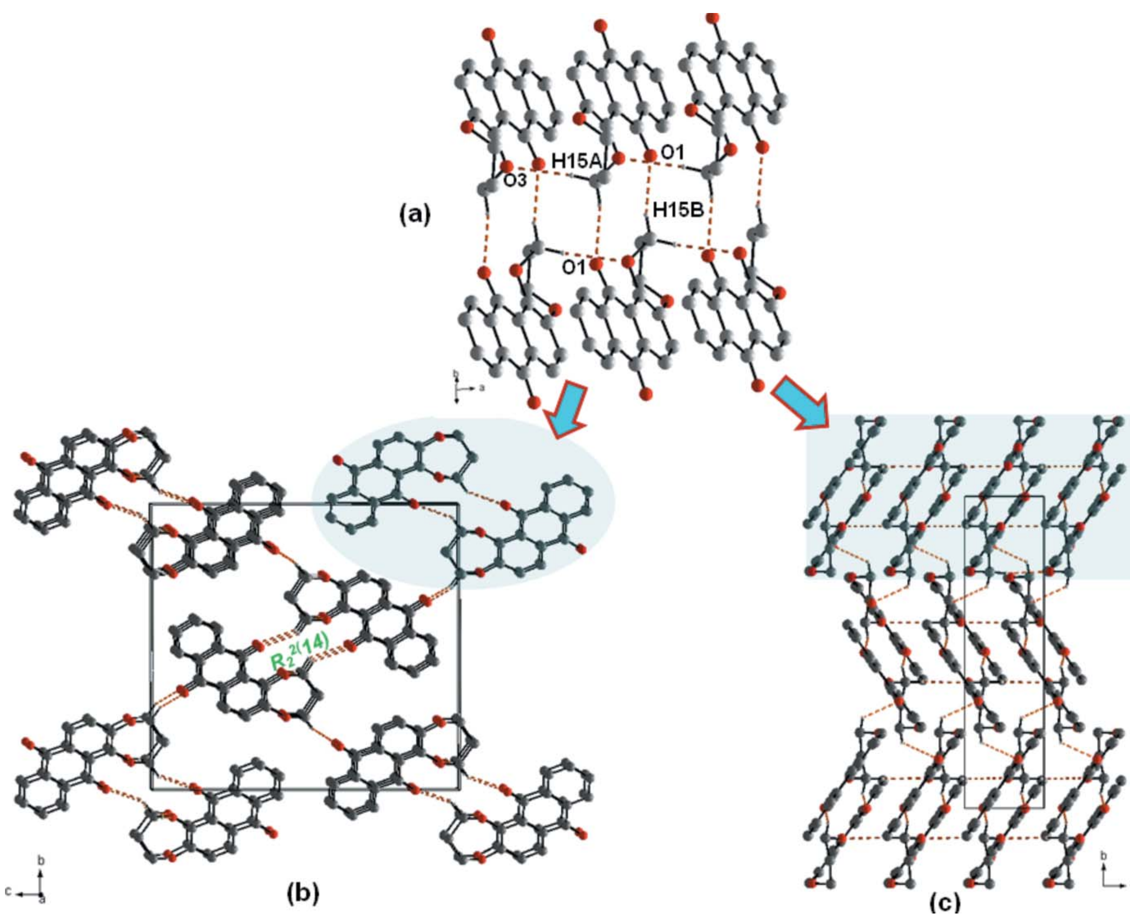

Figure 2
(*a*) Inversion dimers with $R_2^2(14)$ ring motifs; (*b*) and (*c*) packing diagrams of the title compound, viewed along the *a* and *b* axes, respectively. Dotted lines indicate C—H···O hydrogen bonds.

Table 1
Hydrogen-bond geometry (Å, °).

D—H$\cdots$$A$	D—H	H$\cdots$$A$	$D\cdots A$	D—H$\cdots$$A$
C15—H15$B\cdots$O1^{i}	0.99	2.43	3.248 (2)	139
C15—H15$A\cdots$O3^{ii}	0.99	2.48	3.461 (3)	171
C17—H17$A\cdots$O4^{iii}	0.99	2.59	3.580 (3)	174

Symmetry codes: (i) $-x, -y+1, -z+1$; (ii) $x+1, y, z$; (iii) $x-1, y, z$.

thereby generating corrugated chains of molecules (Fig. 2*a*). A C17—H17$B\cdots$O2 hydrogen bond links the chains together (Table 1; Fig. 2*b* and 2*c*), forming sheets propagating in the *ab* plane. These sheets are supported by extensive π–π contacts between adjacent rings, with centroid-to-centroid distances $Cg1\cdots Cg2$ = 3.599 (2) and $Cg2\cdots Cg3$ = 3.683 (2) Å [$Cg1$, $Cg2$ and $Cg3$ are the centroids of the rings C1–C4/C13–C14, C4–C6/C11–C13 and C6–C11, respectively] and weak C12═O1$\cdots\pi$ [oxygen–centroid distance = 3.734 (2) Å] interactions (Fig. 3), linking the slabs to form a three-dimensional supramolecular network.

4. Database survey

A search in the Cambridge Structural Database (CSD, Version 5.40, updated to February 2020; Groom *et al.*, 2016) revealed 55 alizarin-ring motifs incorporated in more complex molecules or bearing functional groups. These include several compounds with a different substituent in place of the dioxepine in the title compound, *viz*. 1-hydroxy-2-methoxy-6-methyl (BOTXUE; Ismail *et al.*, 2009), 1,2-dimethoxy (refcode: KIBHUZ; Kar *et al.*, 2007) and 3-hydroxy-1,2-dimethoxy (BOVVEO; Xu *et al.*, 2009). In these compounds, the anthraquinone ring system are almost planar, the dihedral angle between the benzene rings for BOTXUE, KIBHUZ and BOVVEO being 3.49, 2.83 and 1.12°, respectively. The methoxy groups in position 1 (C14) in KIBHUZ and BOVVEO are almost perpendicular to the anthraquinone ring plane. The other compound belongs to the same class of alizarins with different substituents.

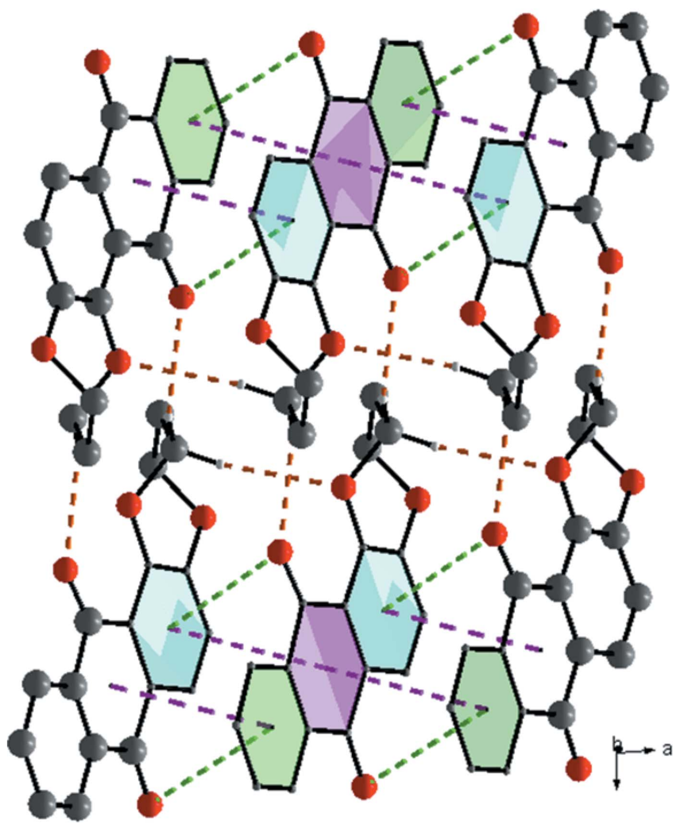

Figure 3
Partial crystal packing for (I) showing the C—H$\cdots$O hydrogen bonds and the offset π–π (purple) and C═O$\cdots\pi$ (green) interactions between inversion-related molecules.

5. Hirshfeld surface analysis

The nature of the intermolecular interactions in (I) have been examined with *CrystalExplorer17.5* (Turner *et al.*, 2017), using Hirshfeld surface analysis (Spackman & Jayatilaka, 2009) mapped over $d_{\rm norm}$, with a fixed colour scale of −0.1779 to 1.3612 a.u (see Fig. S1*a* in the supporting information) and two-dimensional fingerprint plots (McKinnon *et al.*, 2007). The intense red spots on the surface are due to the C—H$\cdots$O hydrogen bonds (Fig. 4). Fig. S2 (supporting information) shows the molecular electrostatic potential surface generated using *TONTO* with a STO-3G basis set in the range −0.050 to

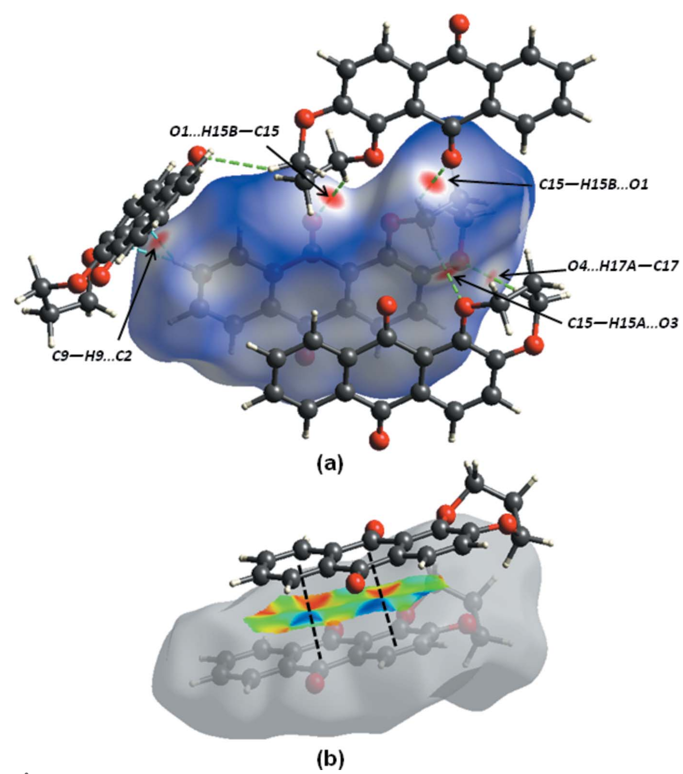

Figure 4
Views of the Hirshfeld surface for (I) mapped over (*a*) $d_{\rm norm}$ showing the C—H$\cdots$O contacts as green dashed lines and short C$\cdots$H/H$\cdots$C contacts as cyan dashed lines; and (*b*) shape-index highlighting the π–π stacking (black lines).

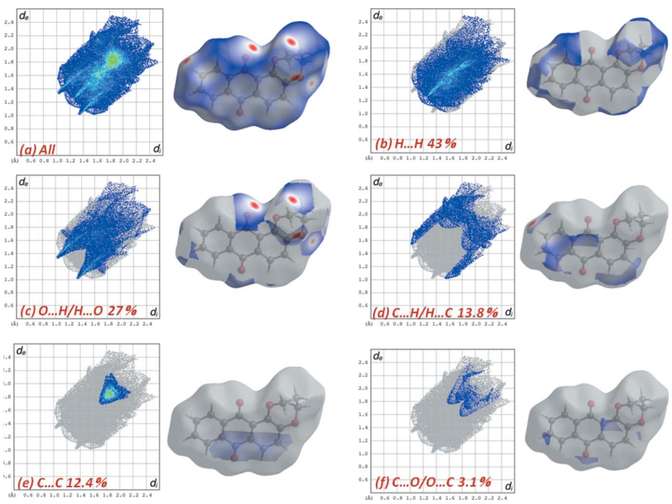

Figure 5
The full two-dimensional fingerprint plots for (I) showing (*a*) all interactions, and delineated into (*b*) H···H, (*c*) H···O/O···H, (*d*) H···C/C···H, (*e*) C···C and (*f*) O···C/C···O interactions.

0.050 a.u. within the Hartree–Fock level of theory. Molecular sites evidenced in red correspond to positive potential energy and in blue to negative potential energy (Spackman *et al.*, 2008).

As illustrated in Fig. 5, the overall fingerprint plot for (I) and those delineated into H···H, H···O/O···H, C···H/H···C and C···C show characteristic pseudo-symmetric wings in the d_e and d_i diagonal axes. The most important interaction is H···H, contributing 43% to the overall crystal packing, which is reflected in Fig. 5*b* as widely scattered points of high density due to the large hydrogen content of the molecule, with small split tips at $d_e \simeq d_i \simeq 1.2$ Å. The contribution from the O···H/H···O contacts (27%) [note that the O···H interactions make a larger contribution (14.6%) than the H···O interactions (12.4%)], corresponding to C—H···O interactions, is represented by a pair of sharp spikes characteristic of a strong hydrogen-bond interaction, $d_e + d_i \simeq 2.35$ Å (Fig. 5*c*). The significant contribution from C···H/H···C contacts (13.8%) to the Hirshfeld surface of (I) reflect the short C···H/H···C contacts, and the distribution of points has characteristic wings, Fig. 5*d*, with $d_e + d_i \simeq 2.55$ Å. The distribution of points in the $d_e = d_i \simeq 1.75$ Å range in the fingerprint plot delineated into C···C contacts indicates the existence of weak π–π stacking interactions between the central anthracene ring and the C6–C11 and C1–C4/C13–C14 rings (Fig. 4*b* and 5*e*). Aromatic π–π interactions are indicated by adjacent red and blue triangles in the shape-index map (Fig. S1*b*)and also by the flat region around these rings in the Hirshfeld surfaces mapped over curvedness in Fig. S1*c*.

The contribution of 3.2% from C···O/O···C contacts is due to the presence of short interatomic C=O···π contacts, and is apparent as the pair of parabolic tips at $d_e + d_i \simeq 3.2$ Å in Fig. 5*f*.

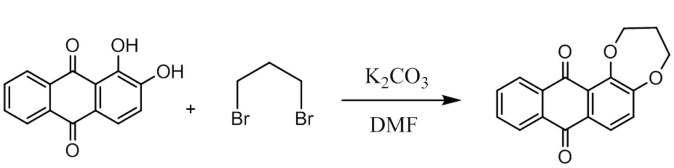

Figure 6
Synthesis pathway leading to the formation of the title compound.

Table 2
Experimental details.

Crystal data	
Chemical formula	$C_{17}H_{12}O_4$
M_r	280.27
Crystal system, space group	Monoclinic, $P2_1/n$
Temperature (K)	173
a, *b*, *c* (Å)	4.2951 (2), 16.7714 (9), 18.0537 (11)
β (°)	95.941 (2)
V (Å^3)	1293.51 (12)
Z	4
Radiation type	Mo $K\alpha$
μ (mm^{-1})	0.10
Crystal size (mm)	0.12 × 0.10 × 0.10
Data collection	
Diffractometer	Bruker APEXII CCD
Absorption correction	Multi-scan (*SADABS*; Bruker, 2012)
T_{min}, T_{max}	0.988, 0.990
No. of measured, independent and observed [$I > 2\sigma(I)$] reflections	19692, 3436, 2309
R_{int}	0.044
$(\sin \theta/\lambda)_{max}$ (Å^{-1})	0.697
Refinement	
$R[F^2 > 2\sigma(F^2)]$, $wR(F^2)$, S	0.055, 0.149, 1.03
No. of reflections	3436
No. of parameters	190
H-atom treatment	H-atom parameters constrained
$\Delta\rho_{max}$, $\Delta\rho_{min}$ (e Å^{-3})	0.41, −0.32

Computer programs: *APEX2* and *SAINT* (Bruker, 2012), *SHELXT2014/5* (Sheldrick, 2015*a*), *SHELXL2018/3* (Sheldrick, 2015*b*), *ORTEP-3 for Windows* (Farrugia, 2012), *DIAMOND* (Brandenburg *et al.*, 2012), *PLATON* (Spek, 2020) and *publCIF* (Westrip, 2010).

6. Synthesis and crystallization

Under argon, alizarin (0.50 g, 2.0 mmol) was treated with 1,3-dibromo-propane (0.42 g, 2.0 mmol) in dimethylformamide (30 ml) in the presence of anhydrous potassium carbonate (1.0 g, 7.2 mmol) with stirring and heated to 393 K for 24 h. The reaction mixture was evaporated to dryness under vacuum and the resulting crude product was acidified with 12 *N* hydrochloric acid, extracted with chloroform (3 × 30 ml) and then chromatographed on a silica gel column with dichloromethane/petroleum ether (1/1) as eluent, which yielded 200 mg (35%) of 1,2-propylenedioxyanthraquinone as a yellow compound (Fig. 6). Colourless needles were obtained by slow evaporation of a dichloromethane/petroleum ether (1:1) solution.

^{1}H NMR (CDCl$_3$, 500 MHz): δ (ppm): 8.21 (*m*, 2H), 7.95 (*d*, J = 8.5 Hz, 1H), 7.72 (*m*, 2H), 7.26 (*d*, J = 8.5 Hz, 1H), 4.48 (*t*, J = 6 Hz, 2H), 4.43 (*t*, J = 6 Hz, 2H), 2.34 (*qt*, J = 6 Hz, 2H); ^{13}C NMR (CDCl$_3$, 126 MHz): δ (ppm): 182.9, 182.5, 157.3, 151.3, 135.2, 133.9, 133.4, 132.6, 129.6, 127.1, 126.5, 126.0, 125.9, 123.3, 70.5, 70.2, 30.0. Analysis calculated for $C_{17}H_{12}O_4$: C, 72.85%; H, 4.32%; found: C, 72.82%; H, 4.29%.

7. Refinement

Crystal data, data collection and structure refinement details are summarized in Table 2. H atoms were placed in calculated positions and refined in the riding model: C—H = 0.95–0.99 Å with $U_{\rm iso}$(H) = 1.2$U_{\rm eq}$(C). The reflection (011), affected by the beam-stop, was removed during refinement.

References

Alves, D. S., Pérez-Fons, L., Estepa, A. & Micol, V. (2004). *Biochem. Pharmacol.* **68**, 549–561.

Brandenburg, K. (2012). *DIAMOND*. *Crystal Impact GbR*, Bonn, Germany.

Bruker (2012). *APEX2*, *SAINT* and *SADABS*. Bruker AXS Inc., Madison, Wisconsin, USA.

Cheuk, D., Svärd, M., Seaton, C., McArdle, P. & Rasmuson, C. (2015). *CrystEngComm*, **17**, 3985–3997.

Czupryniak, J., Niedziałkowski, P., Karbarz, M., Ossowski, T. & Stojek, Z. (2012). *Electroanalysis*, **24**, 975–982.

Farrugia, L. J. (2012). *J. Appl. Cryst.* **45**, 849–854.

Groom, C. R., Bruno, I. J., Lightfoot, M. P. & Ward, S. C. (2016). *Acta Cryst.* B**72**, 171–179.

Ismail, N. H., Osman, C. P., Ahmad, R., Awang, K. & Ng, S. W. (2009). *Acta Cryst.* E**65**, o1435.

Kar, P., Suresh, M., Krishna Kumar, D., Amilan Jose, D., Ganguly, B. & Das, A. (2007). *Polyhedron*, **26**, 1317–1322.

McKinnon, J. J., Jayatilaka, D. & Spackman, M. A. (2007). *Chem. Commun.* pp. 3814–3816.

Nakagawa, H. & Kitamura, C. (2017). *Acta Cryst.* E**73**, 1845–1849.

Okumura, N., Mizutani, H., Ishihama, T., Ito, M., Hashibe, A., Nakayama, T. & Uno, B. (2019). *Chem. Pharm. Bull.* **67**, 717–720.

Oshio, H. & Kawamura, N. (1985). *Shoyakugaku Zasshi*, **39**, 131–138.

Sheldrick, G. M. (2015*a*). *Acta Cryst.* A**71**, 3–8.

Sheldrick, G. M. (2015*b*). *Acta Cryst.* C**71**, 3–8.

Spackman, M. A. & Jayatilaka, D. (2009). *CrystEngComm*, **11**, 19–32.

Spackman, M. A., McKinnon, J. J. & Jayatilaka, D. (2008). *CrystEngComm*, **10**, 377–388.

Spek, A. L. (2020). *Acta Cryst.* E**76**, 1–11.

Tonin, M. D. L., Garden, S. J., Jotani, M. M., Wardell, S. M. S. V., Wardell, J. L. & Tiekink, E. R. T. (2017). *Acta Cryst.* E**73**, 738–745.

Turner, M. J., MacKinnon, J. J., Wolff, S. K., Grimwood, D. J., Spackman, P. R., Jayatilaka, D. & Spackman, M. A. (2017). *Crystal Explorer17.5*. University of Western Australia, Perth, Australia.

Wang, Y., Zhu, K., Zheng, Y., Wang, H., Dong, G., He, N. & Li, Q. (2011). *Molecules*, **16**, 9838–9849.

Westrip, S. P. (2010). *J. Appl. Cryst.* **43**, 920–925.

Xiang, W., Song, Q. S., Zhang, H. J. & Guo, S. P. (2008). *Fitoterapia*, **79**, 501–504.

Xu, Y.-J., Yang, X.-X. & Zhao, H.-B. (2009). *Acta Cryst.* E**65**, o1524.

Yadav, J. P., Arya, V., Yadav, S., Panghal, M., Kumar, S. & Dhankhar, S. (2010). *Fitoterapia*, **81**, 223–230.

Yen, G. C., Duh, P. D. & Chuang, D. Y. (2000). *Food Chem.* **70**, 437–441.

supporting information

Acta Cryst. (2020). E**76**, 576-580 [https://doi.org/10.1107/S2056989020003965]

Crystal structure and Hirshfeld surface analysis of 3,4-dihydro-2*H*-anthra[1,2-*b*][1,4]dioxepine-8,13-dione

Sofia Zazouli, Mohammed Chigr, Ahmed Jouaiti, Nathalie Kyritsakas and El Mostafa Ketatni

Computing details

Data collection: *APEX2* (Bruker, 2012); cell refinement: *SAINT* (Bruker, 2012); data reduction: *SAINT* (Bruker, 2012); program(s) used to solve structure: *SHELXT2014/5* (Sheldrick, 2015*a*); program(s) used to refine structure: *SHELXL2018/3* (Sheldrick, 2015*b*); molecular graphics: *ORTEP-3 for Windows* (Farrugia, 2012) and *DIAMOND* (Brandenburg *et al.*, 2012); software used to prepare material for publication: *PLATON* (Spek, 2020) and *publCIF* (Westrip, 2010).

3,4-Dihydro-2*H*-anthra[1,2-*b*][1,4]dioxepine-8,13-dione

Crystal data

$C_{17}H_{12}O_4$
M_r = 280.27
Monoclinic, $P2_1/n$
a = 4.2951 (2) Å
b = 16.7714 (9) Å
c = 18.0537 (11) Å
β = 95.941 (2)°
V = 1293.51 (12) Å^3
Z = 4
$F(000)$ = 584
D_x = 1.439 Mg m^{-3}
Mo $K\alpha$ radiation, λ = 0.71073 Å
Cell parameters from 3436 reflections
θ = 2.4–29.7°
μ = 0.10 mm^{-1}
T = 173 K
Prism, colorless
0.12 × 0.10 × 0.10 mm

Data collection

Bruker APEXII CCD diffractometer
φ and ω scans
Absorption correction: multi-scan (SADABS; Bruker, 2012)
T_{min} = 0.988, T_{max} = 0.990
19692 measured reflections
3436 independent reflections
2309 reflections with $I > 2\sigma(I)$
R_{int} = 0.044
θ_{max} = 29.7°, θ_{min} = 2.4°
h = −5→4
k = −23→23
l = −24→25

Refinement

Refinement on F^2
Least-squares matrix: full
$R[F^2 > 2\sigma(F^2)]$ = 0.055
$wR(F^2)$ = 0.149
S = 1.02
3436 reflections
190 parameters
0 restraints
Primary atom site location: dual
Hydrogen site location: inferred from neighbouring sites
H-atom parameters constrained
$w = 1/[\sigma^2(F_o^2) + (0.0548P)^2 + 0.8849P]$ where $P = (F_o^2 + 2F_c^2)/3$
$(\Delta/\sigma)_{max}$ < 0.001
$\Delta\rho_{max}$ = 0.41 e Å^{-3}
$\Delta\rho_{min}$ = −0.32 e Å^{-3}

Special details

Geometry. All esds (except the esd in the dihedral angle between two l.s. planes) are estimated using the full covariance matrix. The cell esds are taken into account individually in the estimation of esds in distances, angles and torsion angles; correlations between esds in cell parameters are only used when they are defined by crystal symmetry. An approximate (isotropic) treatment of cell esds is used for estimating esds involving l.s. planes.

Fractional atomic coordinates and isotropic or equivalent isotropic displacement parameters (Å²)

	x	*y*	*z*	$U_{iso}*/U_{eq}$
O1	−0.2635 (5)	0.49906 (10)	0.64736 (8)	0.0546 (5)
O2	0.1717 (4)	0.34277 (9)	0.89646 (7)	0.0449 (4)
O3	0.0471 (3)	0.40325 (8)	0.56747 (6)	0.0293 (3)
O4	0.4204 (4)	0.25897 (8)	0.56830 (7)	0.0356 (3)
C1	0.3367 (5)	0.29496 (11)	0.63141 (10)	0.0274 (4)
C2	0.4523 (5)	0.26018 (11)	0.69817 (11)	0.0321 (4)
H2	0.590316	0.215932	0.697909	0.038*
C3	0.3704 (5)	0.28874 (11)	0.76486 (10)	0.0302 (4)
H3	0.451085	0.264092	0.810209	0.036*
C4	0.1701 (4)	0.35347 (10)	0.76600 (9)	0.0244 (4)
C5	0.0822 (5)	0.37964 (11)	0.83960 (10)	0.0285 (4)
C6	−0.1143 (5)	0.45162 (10)	0.84226 (9)	0.0269 (4)
C7	−0.1904 (5)	0.47948 (12)	0.91105 (10)	0.0351 (5)
H7	−0.121046	0.451264	0.955331	0.042*
C8	−0.3662 (6)	0.54788 (13)	0.91472 (11)	0.0407 (5)
H8	−0.413992	0.567394	0.961621	0.049*
C9	−0.4731 (5)	0.58819 (12)	0.85004 (11)	0.0377 (5)
H9	−0.595642	0.635045	0.852781	0.045*
C10	−0.4023 (5)	0.56056 (11)	0.78134 (11)	0.0308 (4)
H10	−0.478159	0.588130	0.737151	0.037*
C11	−0.2198 (4)	0.49227 (10)	0.77718 (9)	0.0248 (4)
C12	−0.1467 (5)	0.46397 (10)	0.70231 (9)	0.0271 (4)
C13	0.0595 (4)	0.39292 (10)	0.69919 (9)	0.0227 (4)
C14	0.1495 (4)	0.36425 (10)	0.63107 (9)	0.0238 (4)
C15	0.2543 (5)	0.40456 (12)	0.50847 (10)	0.0331 (4)
H15A	0.474823	0.405280	0.530766	0.040*
H15B	0.216063	0.453607	0.478396	0.040*
C16	0.1997 (6)	0.33217 (13)	0.45871 (11)	0.0389 (5)
H16A	0.001584	0.338786	0.426047	0.047*
H16B	0.372274	0.327239	0.426649	0.047*
C17	0.1829 (6)	0.25735 (13)	0.50493 (11)	0.0384 (5)
H17A	−0.026930	0.253140	0.522692	0.046*
H17B	0.214839	0.210027	0.473818	0.046*

Atomic displacement parameters (Å²)

	U^{11}	U^{22}	U^{33}	U^{12}	U^{13}	U^{23}
O1	0.0835 (14)	0.0550 (10)	0.0254 (7)	0.0370 (9)	0.0062 (8)	0.0053 (6)
O2	0.0590 (12)	0.0499 (9)	0.0257 (7)	0.0106 (8)	0.0036 (7)	0.0110 (6)

O3	0.0301 (8)	0.0378 (7)	0.0201 (6)	0.0062 (6)	0.0029 (5)	0.0009 (5)
O4	0.0345 (9)	0.0386 (8)	0.0346 (7)	0.0062 (6)	0.0078 (6)	−0.0075 (6)
C1	0.0248 (10)	0.0272 (9)	0.0307 (9)	−0.0022 (7)	0.0053 (7)	−0.0040 (7)
C2	0.0296 (11)	0.0267 (9)	0.0394 (10)	0.0036 (7)	0.0010 (8)	0.0015 (7)
C3	0.0297 (11)	0.0283 (9)	0.0313 (9)	0.0005 (7)	−0.0030 (8)	0.0054 (7)
C4	0.0245 (10)	0.0230 (8)	0.0252 (8)	−0.0033 (7)	0.0002 (7)	0.0022 (6)
C5	0.0314 (11)	0.0298 (9)	0.0237 (8)	−0.0042 (7)	0.0002 (7)	0.0022 (7)
C6	0.0309 (11)	0.0278 (8)	0.0220 (8)	−0.0070 (7)	0.0025 (7)	−0.0014 (6)
C7	0.0445 (14)	0.0376 (10)	0.0238 (9)	−0.0053 (9)	0.0064 (8)	−0.0010 (7)
C8	0.0538 (16)	0.0407 (11)	0.0295 (10)	−0.0035 (10)	0.0143 (9)	−0.0078 (8)
C9	0.0429 (14)	0.0317 (10)	0.0402 (11)	0.0007 (9)	0.0126 (9)	−0.0054 (8)
C10	0.0342 (12)	0.0264 (9)	0.0322 (9)	−0.0008 (7)	0.0054 (8)	−0.0002 (7)
C11	0.0274 (10)	0.0233 (8)	0.0239 (8)	−0.0051 (7)	0.0027 (7)	−0.0011 (6)
C12	0.0304 (11)	0.0274 (9)	0.0234 (8)	0.0015 (7)	0.0015 (7)	0.0006 (6)
C13	0.0233 (10)	0.0213 (8)	0.0231 (8)	−0.0039 (6)	0.0010 (6)	0.0006 (6)
C14	0.0218 (10)	0.0255 (8)	0.0236 (8)	−0.0033 (7)	0.0005 (7)	−0.0003 (6)
C15	0.0353 (12)	0.0407 (11)	0.0246 (9)	0.0002 (8)	0.0085 (8)	0.0014 (7)
C16	0.0396 (14)	0.0525 (12)	0.0256 (9)	0.0027 (10)	0.0080 (8)	−0.0079 (8)
C17	0.0376 (13)	0.0428 (11)	0.0357 (10)	−0.0027 (9)	0.0078 (9)	−0.0145 (8)

Geometric parameters (Å, º)

O1—C12	1.216 (2)	C7—H7	0.9500
O2—C5	1.226 (2)	C8—C9	1.386 (3)
O3—C14	1.355 (2)	C8—H8	0.9500
O3—C15	1.457 (2)	C9—C10	1.387 (3)
O4—C1	1.370 (2)	C9—H9	0.9500
O4—C17	1.452 (3)	C10—C11	1.394 (3)
C1—C2	1.384 (3)	C10—H10	0.9500
C1—C14	1.413 (3)	C11—C12	1.496 (2)
C2—C3	1.375 (3)	C12—C13	1.489 (2)
C2—H2	0.9500	C13—C14	1.411 (2)
C3—C4	1.387 (3)	C15—C16	1.514 (3)
C3—H3	0.9500	C15—H15A	0.9900
C4—C13	1.414 (2)	C15—H15B	0.9900
C4—C5	1.485 (2)	C16—C17	1.513 (3)
C5—C6	1.477 (3)	C16—H16A	0.9900
C6—C11	1.393 (2)	C16—H16B	0.9900
C6—C7	1.397 (2)	C17—H17A	0.9900
C7—C8	1.379 (3)	C17—H17B	0.9900
C14—O3—C15	117.23 (15)	C11—C10—H10	120.0
C1—O4—C17	116.12 (16)	C6—C11—C10	119.49 (16)
O4—C1—C2	115.92 (17)	C6—C11—C12	121.76 (16)
O4—C1—C14	123.85 (16)	C10—C11—C12	118.75 (15)
C2—C1—C14	120.22 (16)	O1—C12—C13	123.57 (16)
C3—C2—C1	120.95 (18)	O1—C12—C11	118.43 (17)
C3—C2—H2	119.5	C13—C12—C11	117.99 (14)

C1—C2—H2	119.5	C14—C13—C4	119.06 (16)
C2—C3—C4	120.08 (17)	C14—C13—C12	121.55 (15)
C2—C3—H3	120.0	C4—C13—C12	119.39 (15)
C4—C3—H3	120.0	O3—C14—C13	118.68 (15)
C3—C4—C13	120.52 (16)	O3—C14—C1	122.38 (15)
C3—C4—C5	117.40 (15)	C13—C14—C1	118.92 (15)
C13—C4—C5	122.07 (16)	O3—C15—C16	110.66 (16)
O2—C5—C6	121.06 (17)	O3—C15—H15A	109.5
O2—C5—C4	120.92 (18)	C16—C15—H15A	109.5
C6—C5—C4	118.02 (15)	O3—C15—H15B	109.5
C11—C6—C7	120.04 (18)	C16—C15—H15B	109.5
C11—C6—C5	120.65 (16)	H15A—C15—H15B	108.1
C7—C6—C5	119.31 (16)	C17—C16—C15	110.55 (16)
C8—C7—C6	120.04 (18)	C17—C16—H16A	109.5
C8—C7—H7	120.0	C15—C16—H16A	109.5
C6—C7—H7	120.0	C17—C16—H16B	109.5
C7—C8—C9	120.06 (18)	C15—C16—H16B	109.5
C7—C8—H8	120.0	H16A—C16—H16B	108.1
C9—C8—H8	120.0	O4—C17—C16	110.46 (18)
C8—C9—C10	120.42 (19)	O4—C17—H17A	109.6
C8—C9—H9	119.8	C16—C17—H17A	109.6
C10—C9—H9	119.8	O4—C17—H17B	109.6
C9—C10—C11	119.94 (18)	C16—C17—H17B	109.6
C9—C10—H10	120.0	H17A—C17—H17B	108.1

Hydrogen-bond geometry (Å, º)

D—H···*A*	*D*—H	H···*A*	*D*···*A*	*D*—H···*A*
C15—H15*B*···O1^{i}	0.99	2.43	3.248 (2)	139
C15—H15*A*···O3^{ii}	0.99	2.48	3.461 (3)	171
C17—H17*A*···O4^{iii}	0.99	2.59	3.580 (3)	174

Symmetry codes: (i) $-x$, $-y+1$, $-z+1$; (ii) $x+1$, y, z; (iii) $x-1$, y, z.